


The need for Ni/Co-free Li-ion cathodes


- Current **Nickel** and **Cobalt** supply chains insecure & dominated by foreign interests.
- More **Cobalt** needed to meet 2050 demand than currently exists on Earth.

Nickel Production



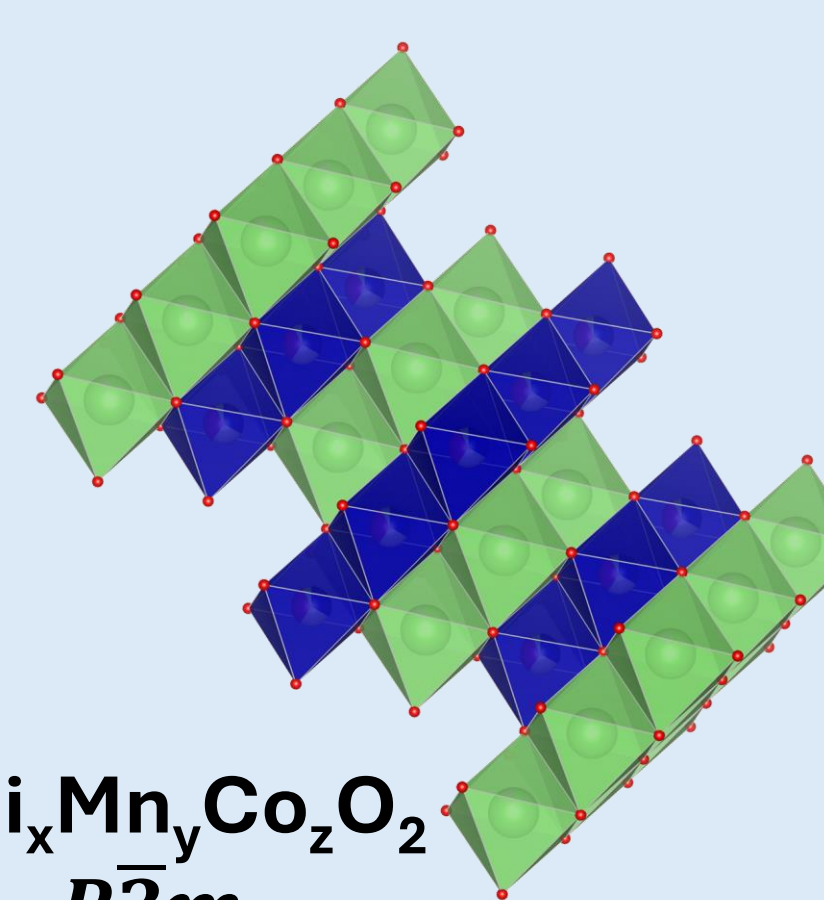
50% of global **Nickel** production comes from **Indonesia**

Cobalt Production

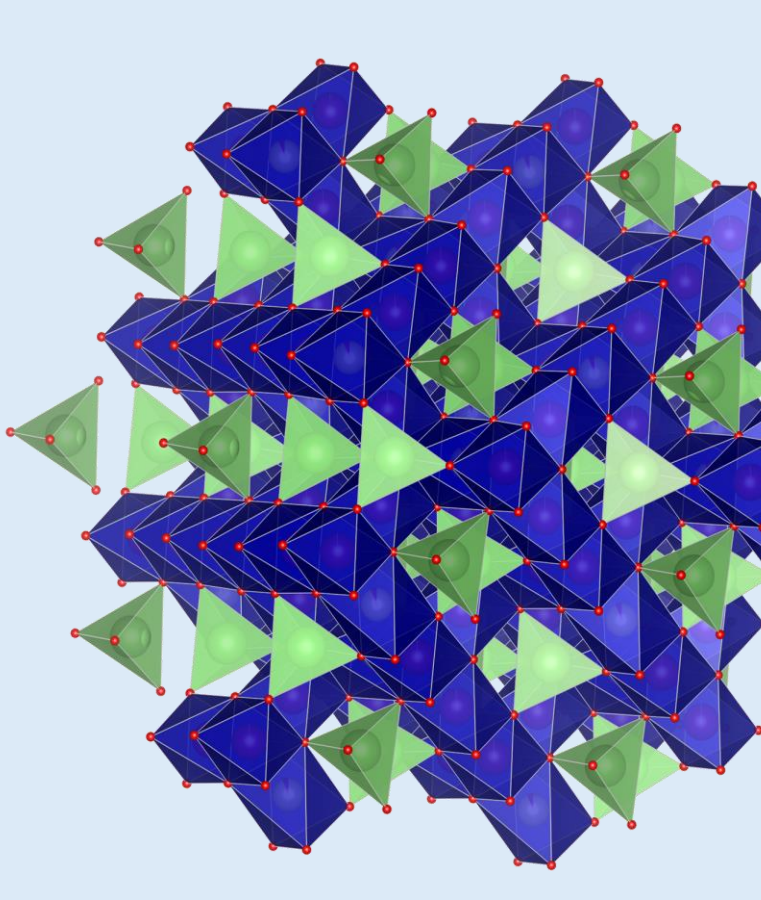


71% of global **Cobalt** production comes from the **DRC**

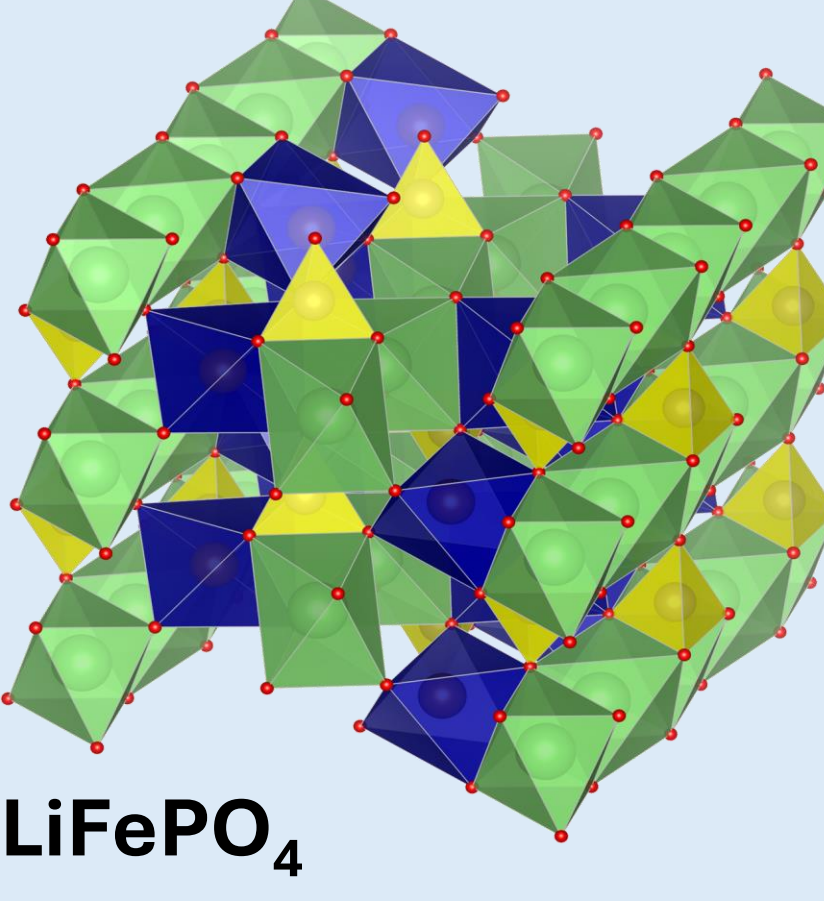
Conventional cathode chemistries



$\text{LiNi}_x\text{Mn}_y\text{Co}_z\text{O}_2$
R3m



$\text{LiMn}_{2-x}\text{Ni}_x\text{O}_4$
P4₃32

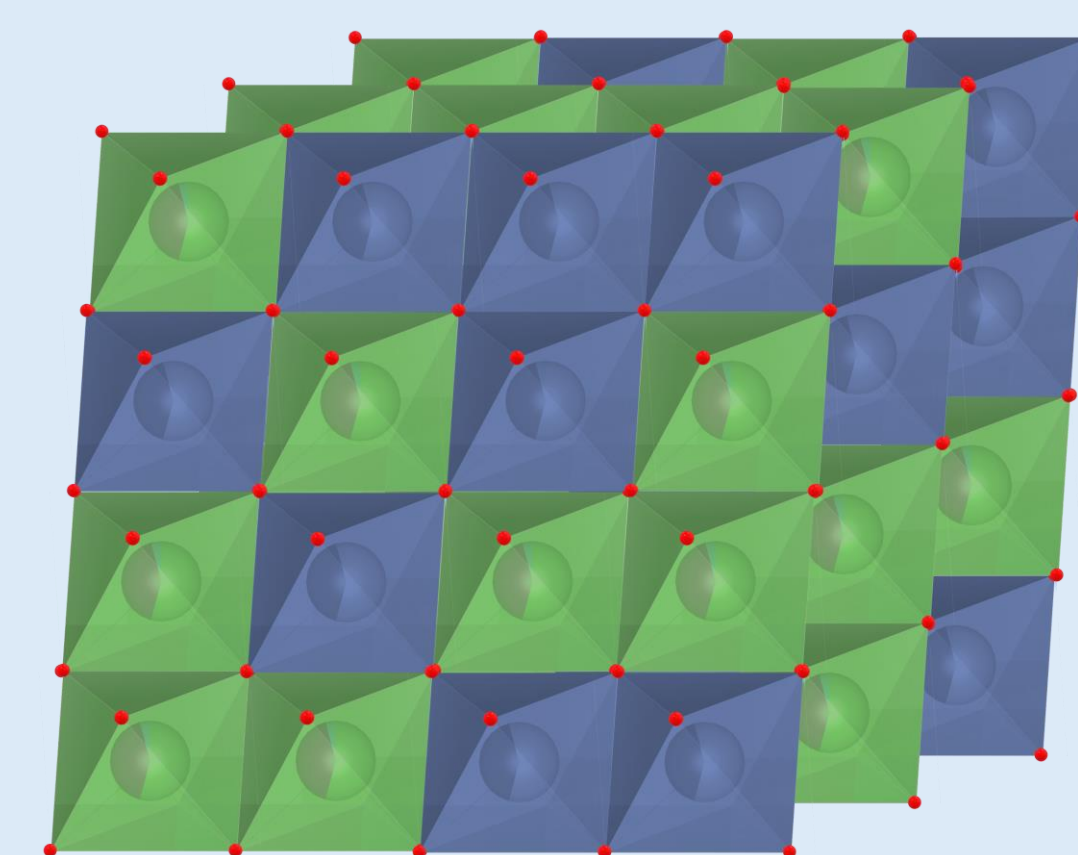


LiFePO_4
Pnma

Legend:

- Lithium
- Transition Metals (TMs)
- Phosphorous
- Oxygen

Disordered Rocksalt Oxyfluorides



Randomly disordered cations (TM and Li)

Benefits:

- Enables higher specific energy (more Li⁺ per kg).
- Utilizes a distribution of Li-TM channels.
- Can rely on more earth abundant TMs (NOT limited to Ni and/or Co).

Issues:

- Short range ordering (SRO) can block Li transport.
- Low electronic conductivity.
- Complex morphology requires higher carbon content in cathode.

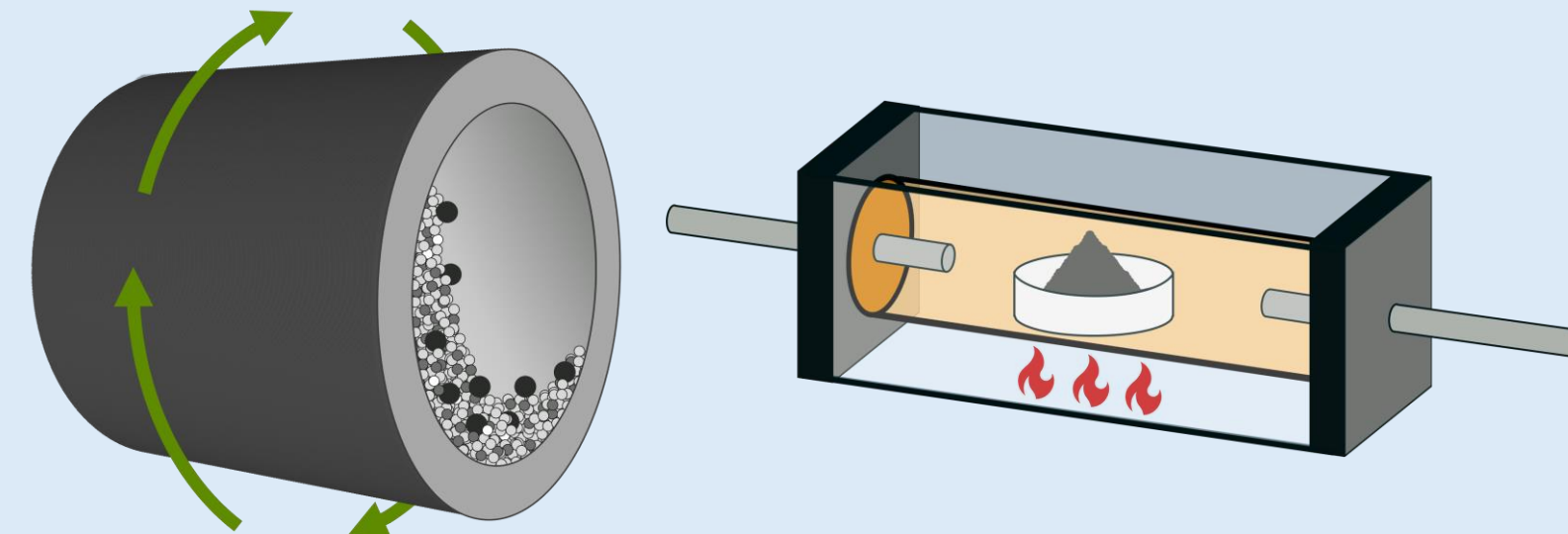
TM-0 **TM-1**

Lithium-ion conducting TM channels

TM-2 **TM-3** **TM-4**

Non-Lithium-ion conducting TM channels

Motivation



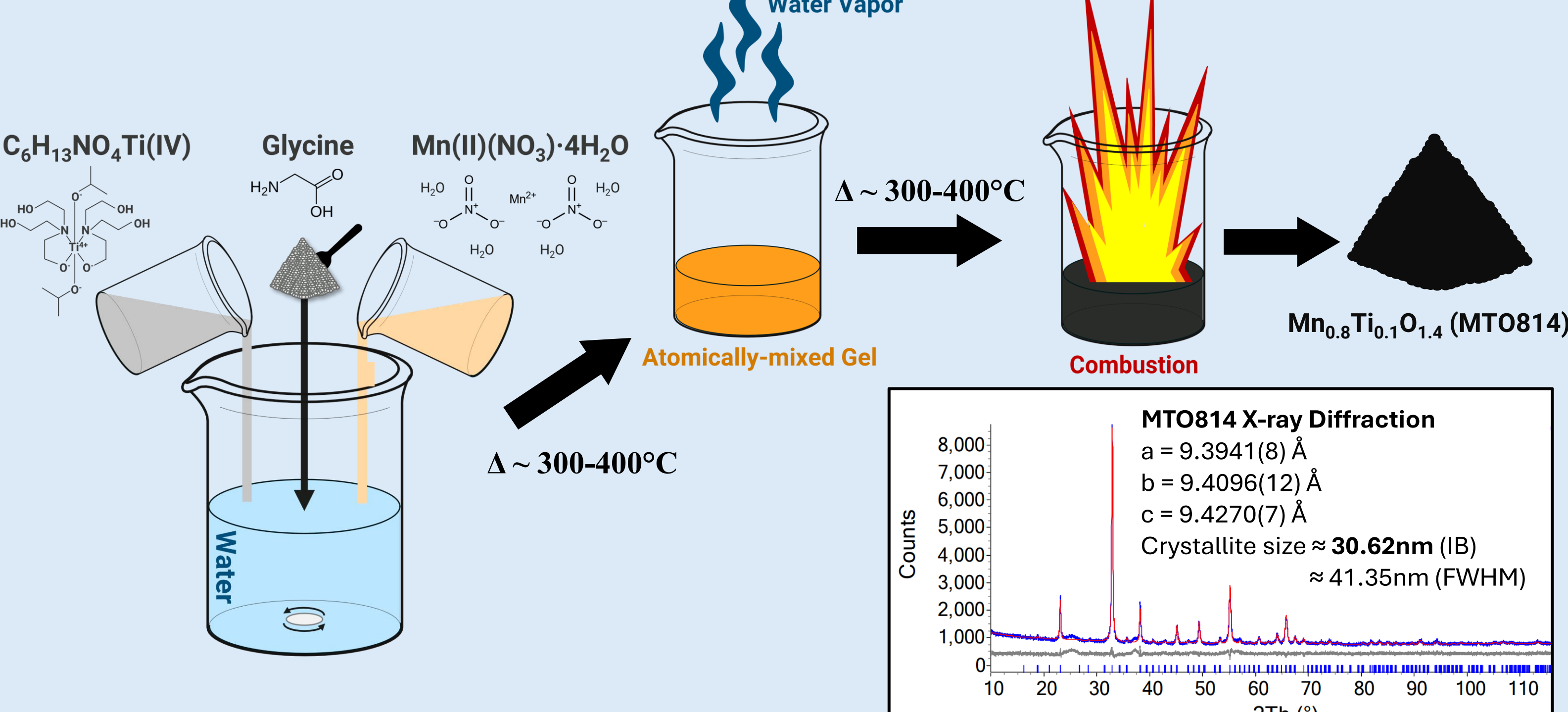
- Conventional DRX synthesis relies on **high energy ball milling** and **long reactions at high temperature** (up to 12h at 1000°C)
- Yields **high phase purity** but offers **no morphology control**.
- Unable to effectively fluorine substitute oxygen sites.
- Higher Mn concentrations more difficult to synthesize due to energy required to produce Mn-F bonds.
- Is **difficult to scale** for commercial application.

Alternative synthesis methods needed!

Combustion synthesis offers alternative that is **compositionally precise**, **can control morphology**, and is **very scalable**.

Synthesis Method Part I: Combustion Synthesis of Mn/Ti Oxide Precursor

$\text{C}_6\text{H}_{13}\text{NO}_4\text{Ti(IV)}$
Glycine
 $\text{Mn(II)(NO}_3)_4 \cdot 4\text{H}_2\text{O}$



Water Vapor

Atomically-mixed Gel

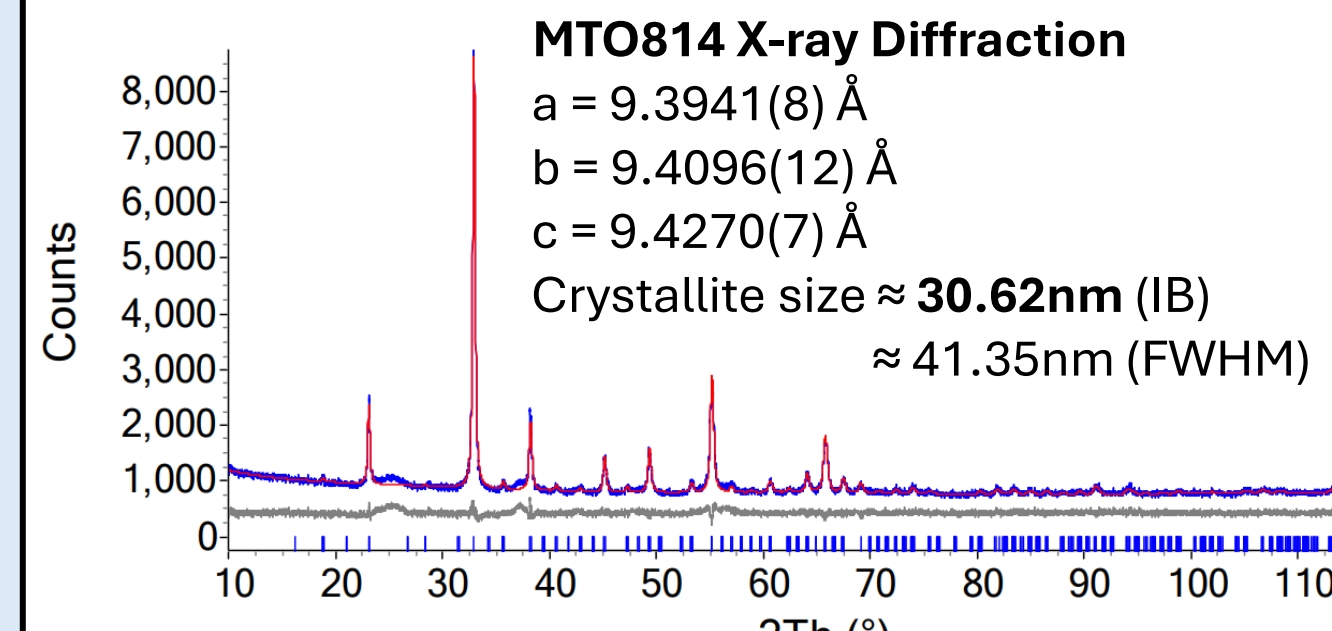
Combustion

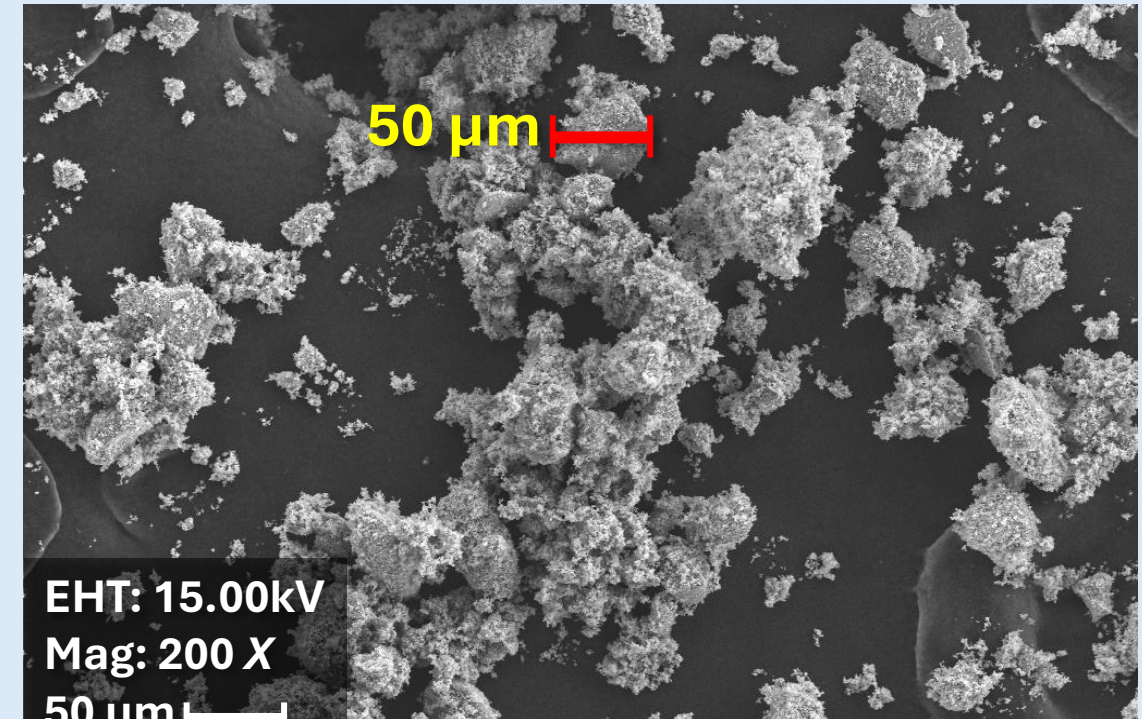
$\text{Mn}_{0.8}\text{Ti}_{0.1}\text{O}_{1.4}$ (MT0814)

$\Delta \sim 300\text{--}400^\circ\text{C}$

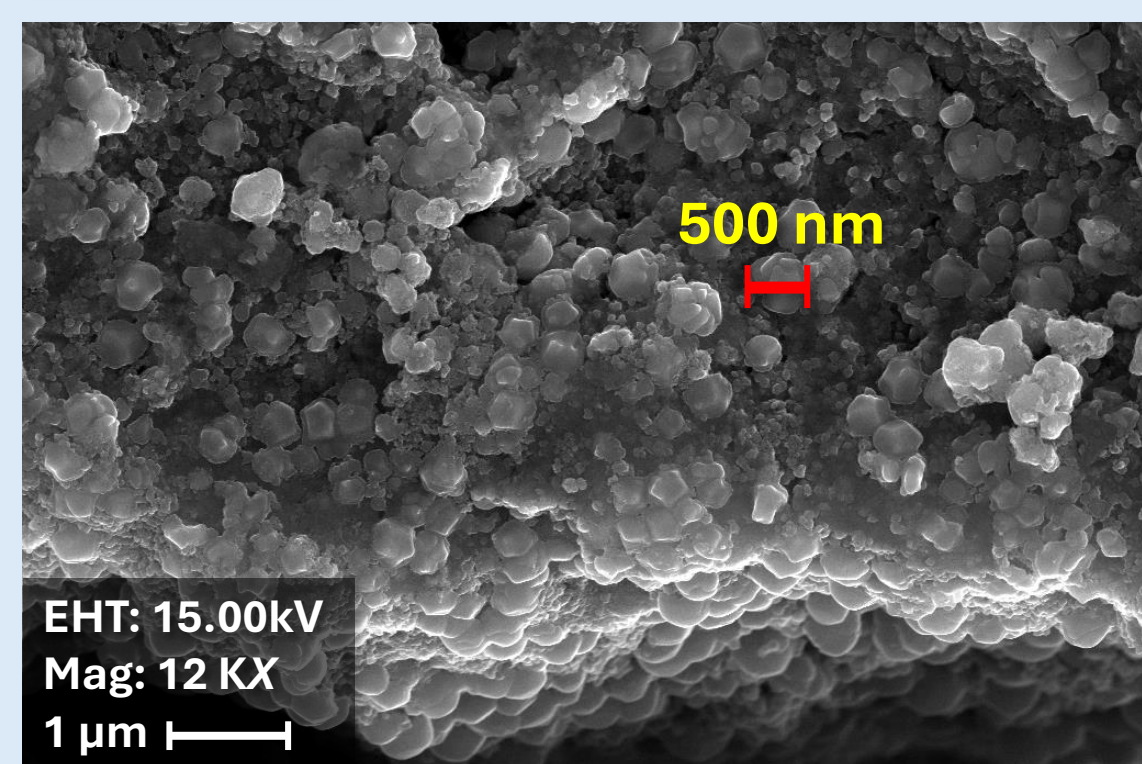
MT0814 X-ray Diffraction

$a = 9.3941(8) \text{ \AA}$
 $b = 9.4096(12) \text{ \AA}$
 $c = 9.4270(7) \text{ \AA}$
 Crystallite size $\approx 30.62\text{nm}$ (IB)
 $\approx 41.35\text{nm}$ (FWHM)





EHT: 15.00kV
Mag: 200 X
50 μm

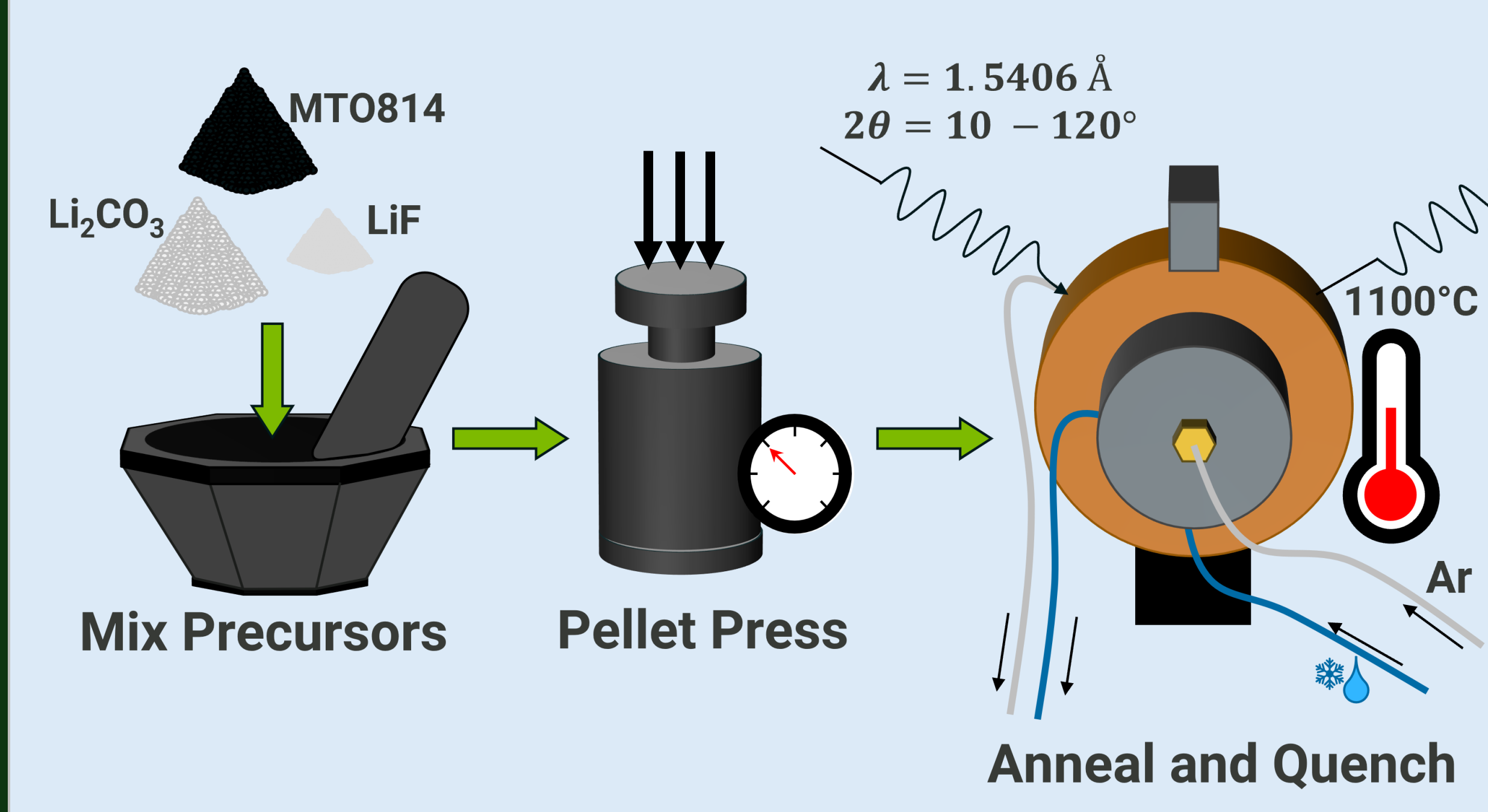


EHT: 15.00kV
Mag: 12 KX
1 μm

Synthesis Method Part II: Solid-State Synthesis of DRX

MT0814

Li_2CO_3 LiF



Mix Precursors

Pellet Press

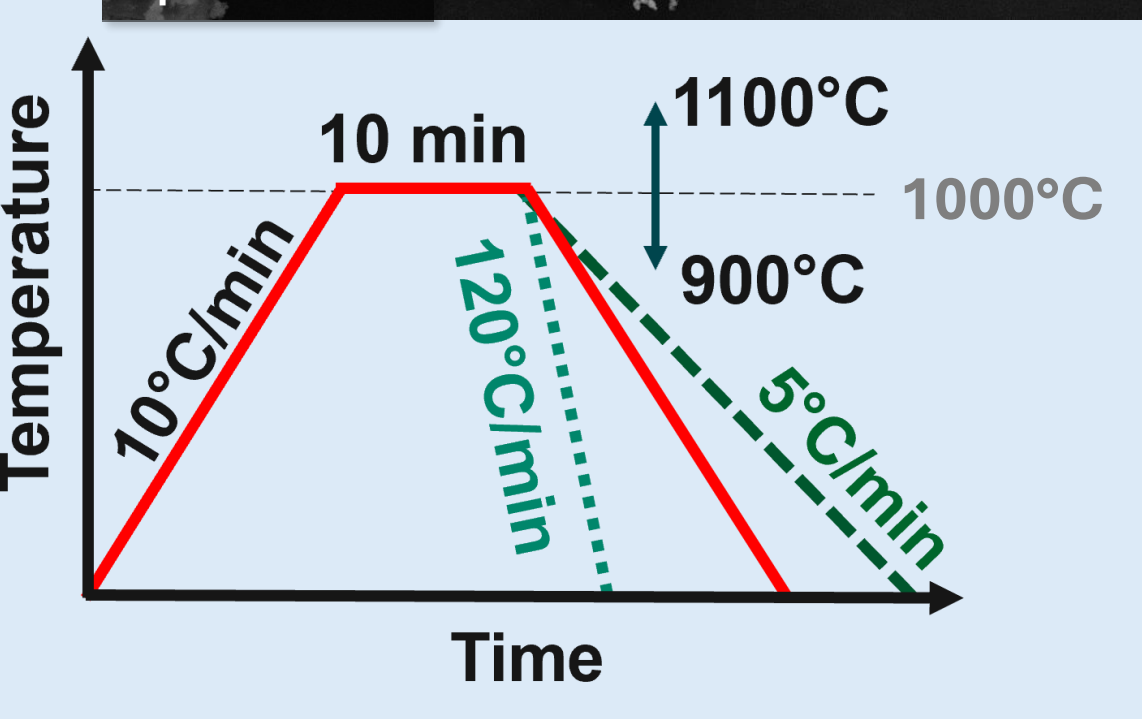
Anneal and Quench

$\lambda = 1.5406 \text{ \AA}$
 $2\theta = 10 - 120^\circ$

1100°C

Ar

Temperature vs Time



10°C/min

10 min

1100°C

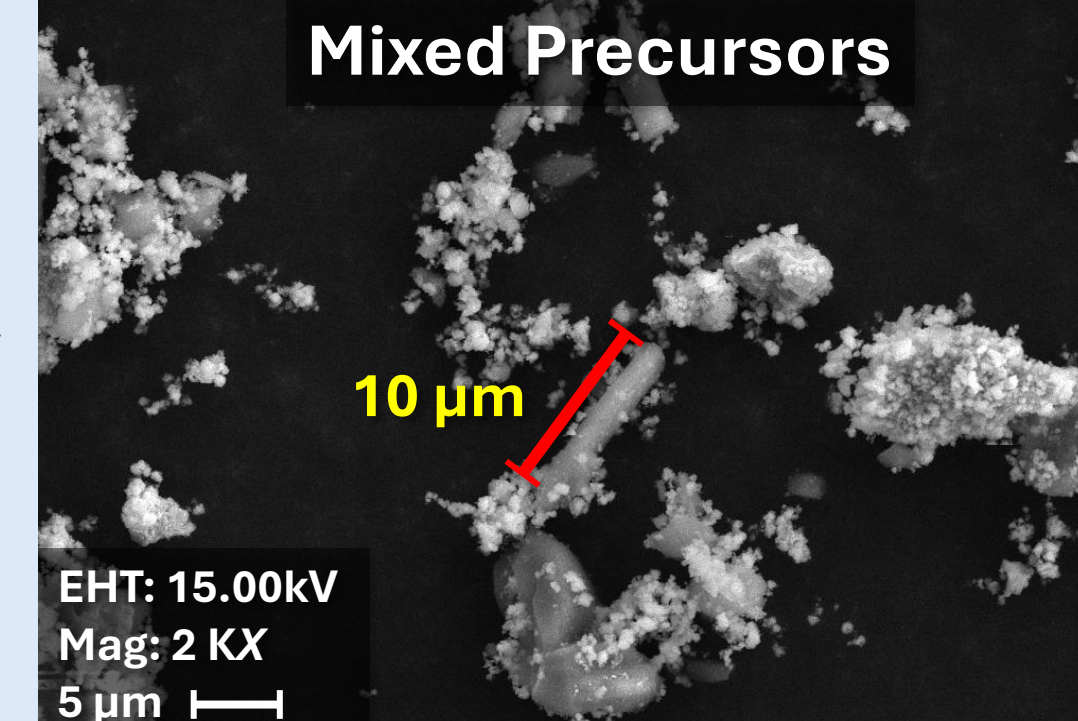
120°C/min

900°C

5°C/min

1000°C

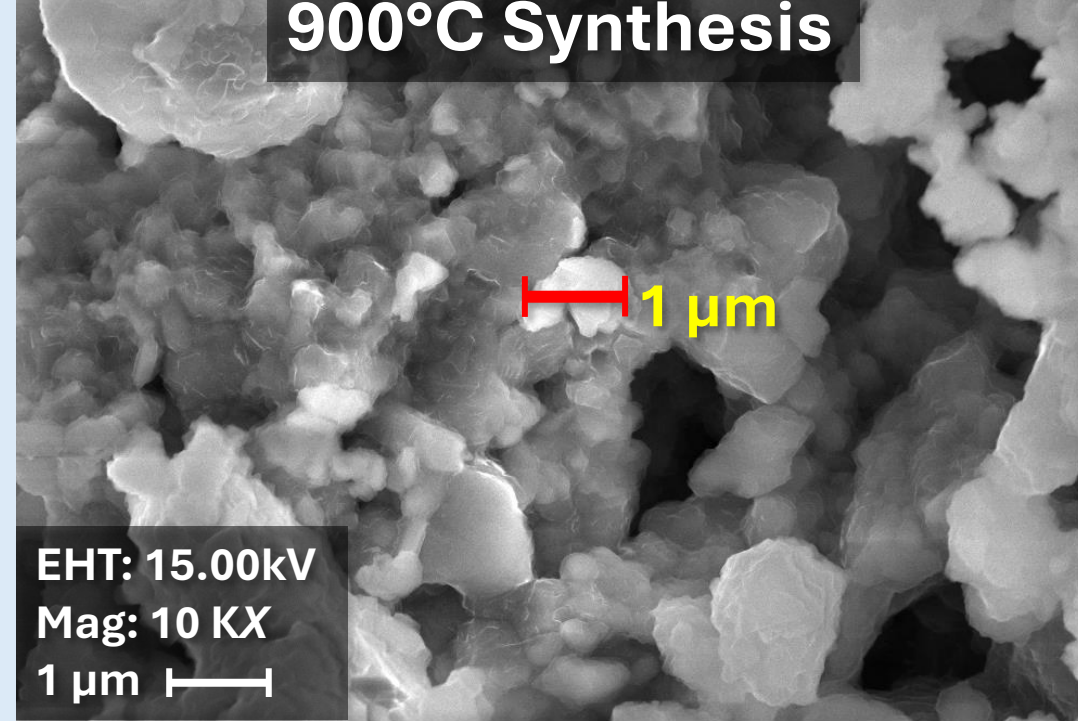
Mixed Precursors



EHT: 15.00kV
Mag: 2 KX
5 μm

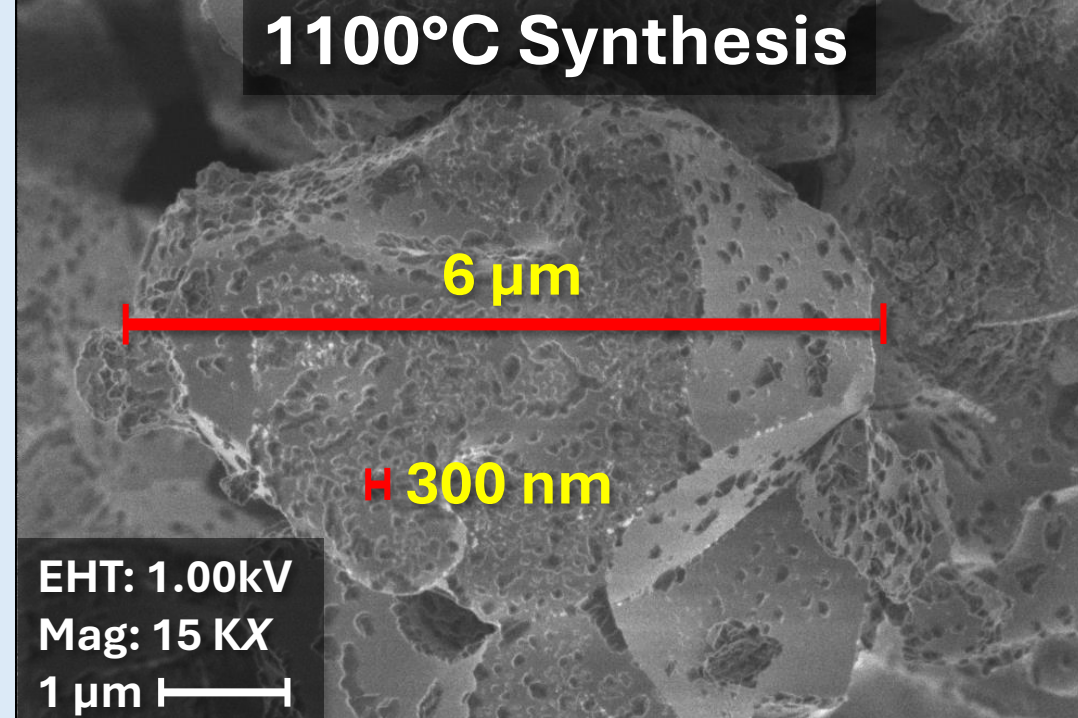
Annealing Temperature Dependence

900°C Synthesis



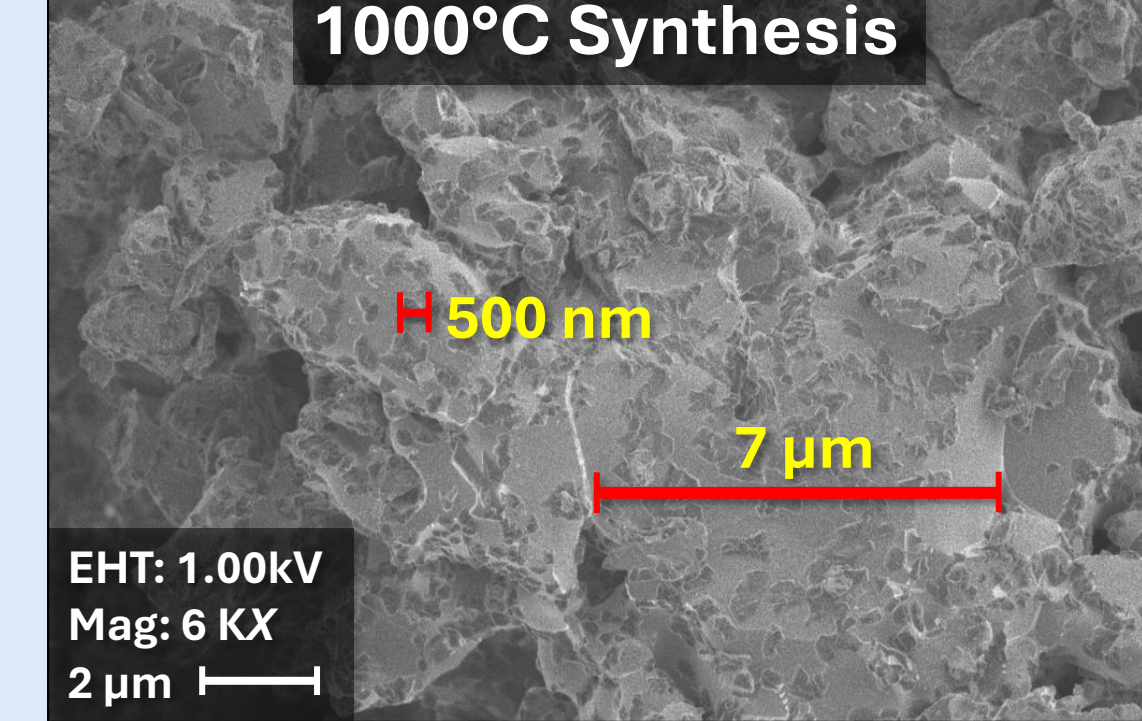
EHT: 15.00kV
Mag: 10 KX
1 μm

1100°C Synthesis



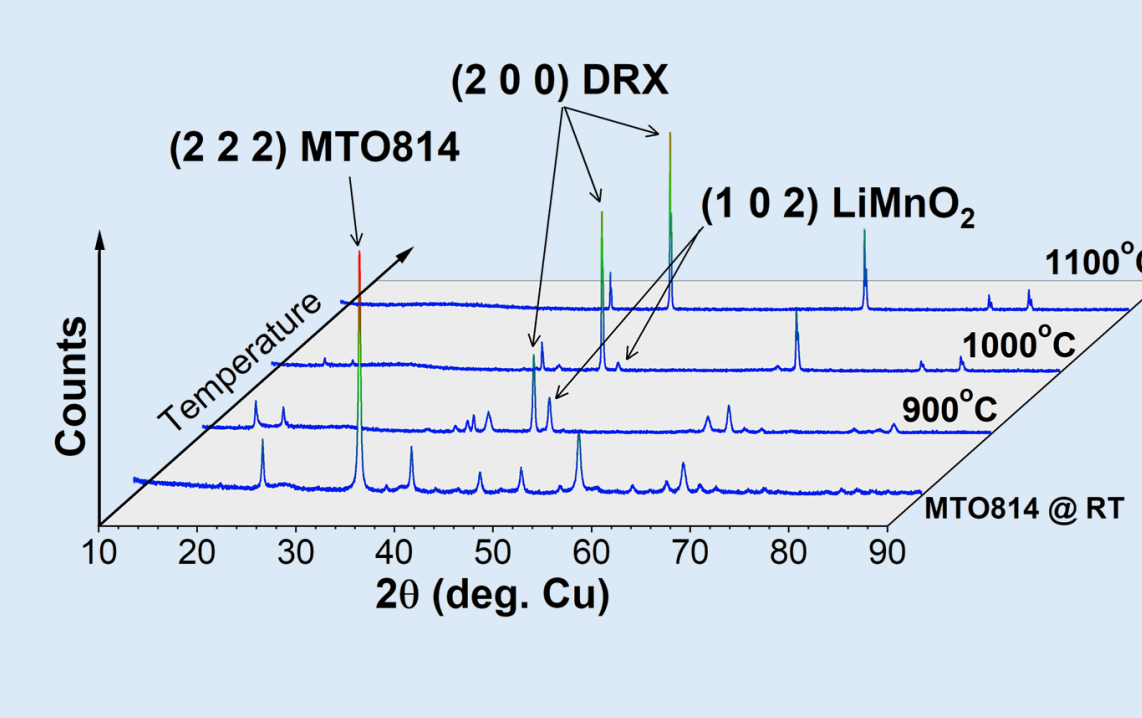
EHT: 1.00kV
Mag: 15 KX
1 μm

1000°C Synthesis



EHT: 1.00kV
Mag: 6 KX
2 μm

XRD Patterns



(2 0 0) DRX

(2 2 2) MT0814

(1 0 2) LiMnO₂

Counts

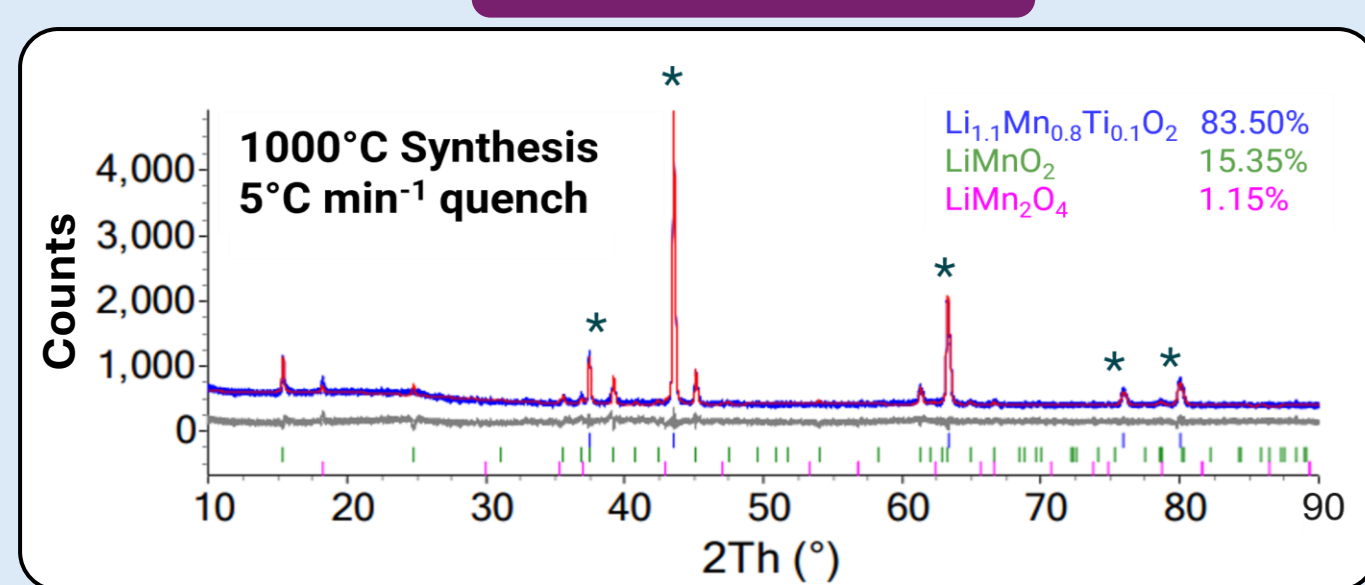
Temperature

2 θ (deg. Cu)

Quench Rate Dependence

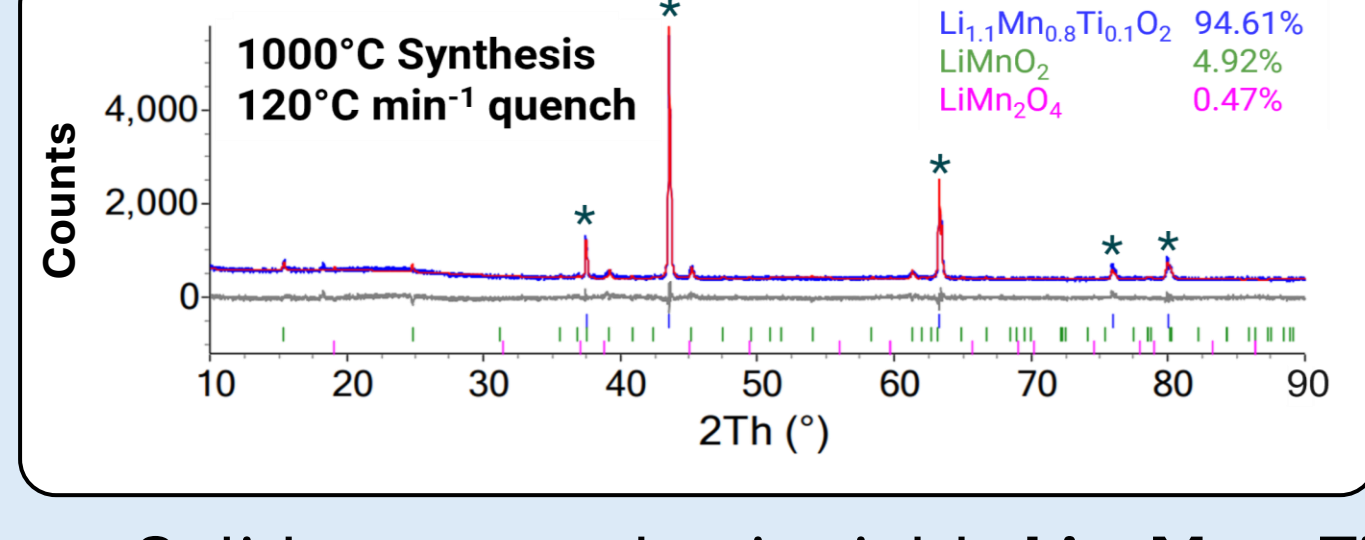
1000°C Synthesis

1000°C Synthesis 5°C min⁻¹ quench



$\text{Li}_{1.1}\text{Mn}_{0.8}\text{Ti}_{0.1}\text{O}_{1.9}\text{F}_{0.1}$ 83.50%
 LiMnO_2 15.35%
 LiMn_2O_4 1.15%

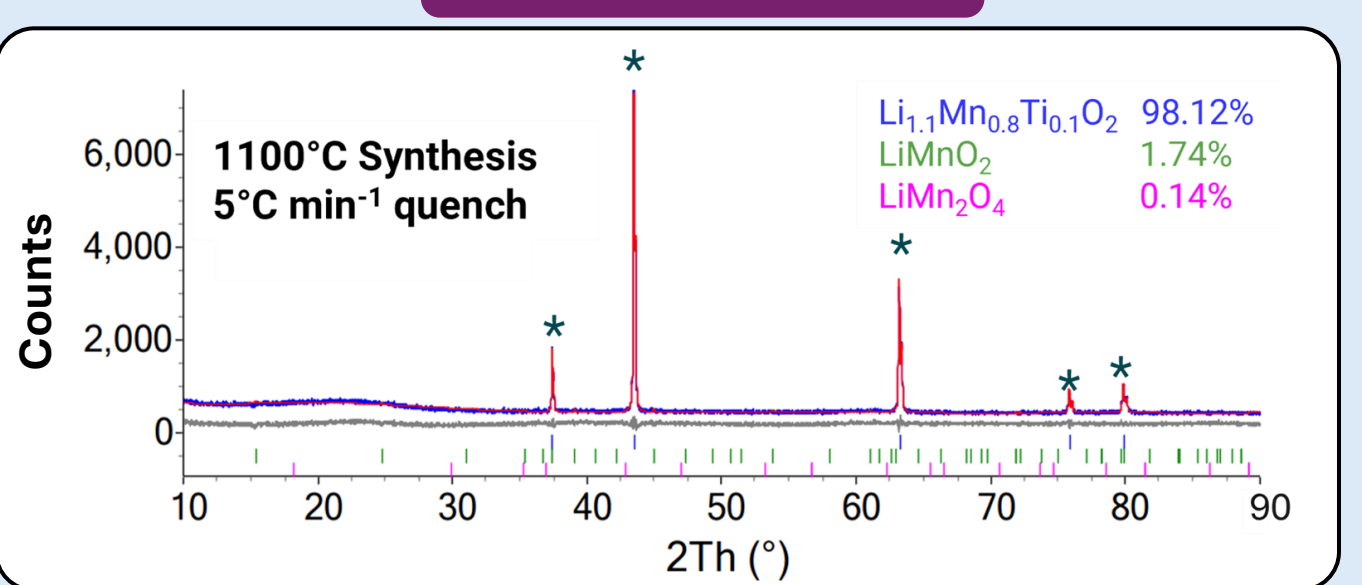
1000°C Synthesis 120°C min⁻¹ quench



$\text{Li}_{1.1}\text{Mn}_{0.8}\text{Ti}_{0.1}\text{O}_{1.9}\text{F}_{0.1}$ 94.61%
 LiMnO_2 4.92%
 LiMn_2O_4 0.47%

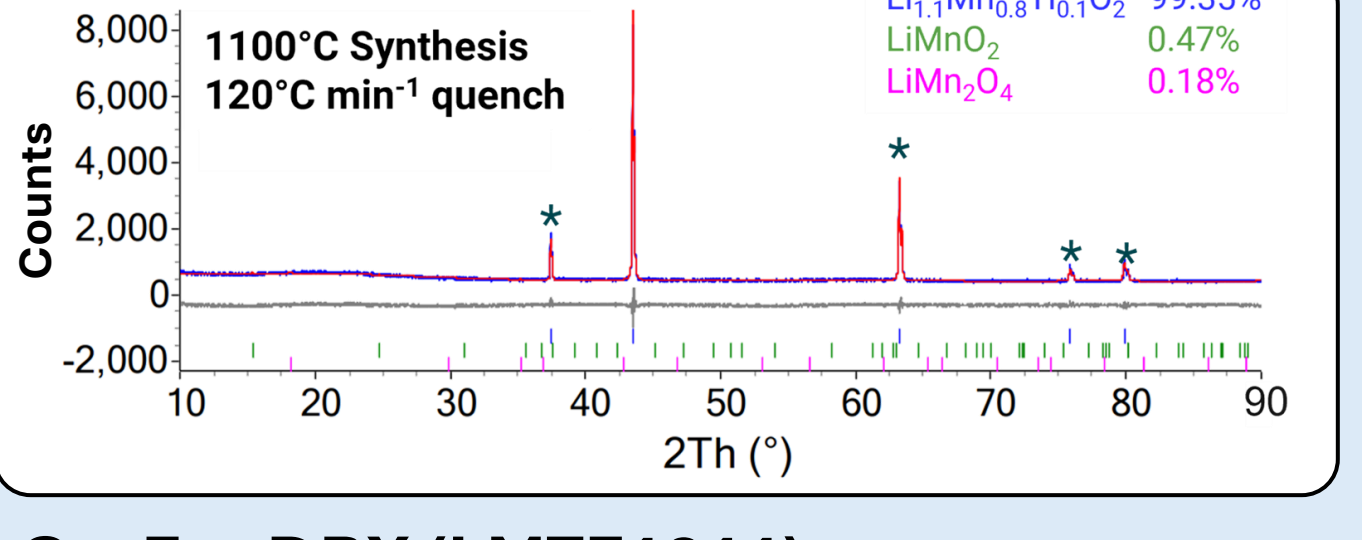
1100°C Synthesis

1100°C Synthesis 5°C min⁻¹ quench



$\text{Li}_{1.1}\text{Mn}_{0.8}\text{Ti}_{0.1}\text{O}_{1.9}\text{F}_{0.1}$ 98.12%
 LiMnO_2 1.74%
 LiMn_2O_4 0.14%

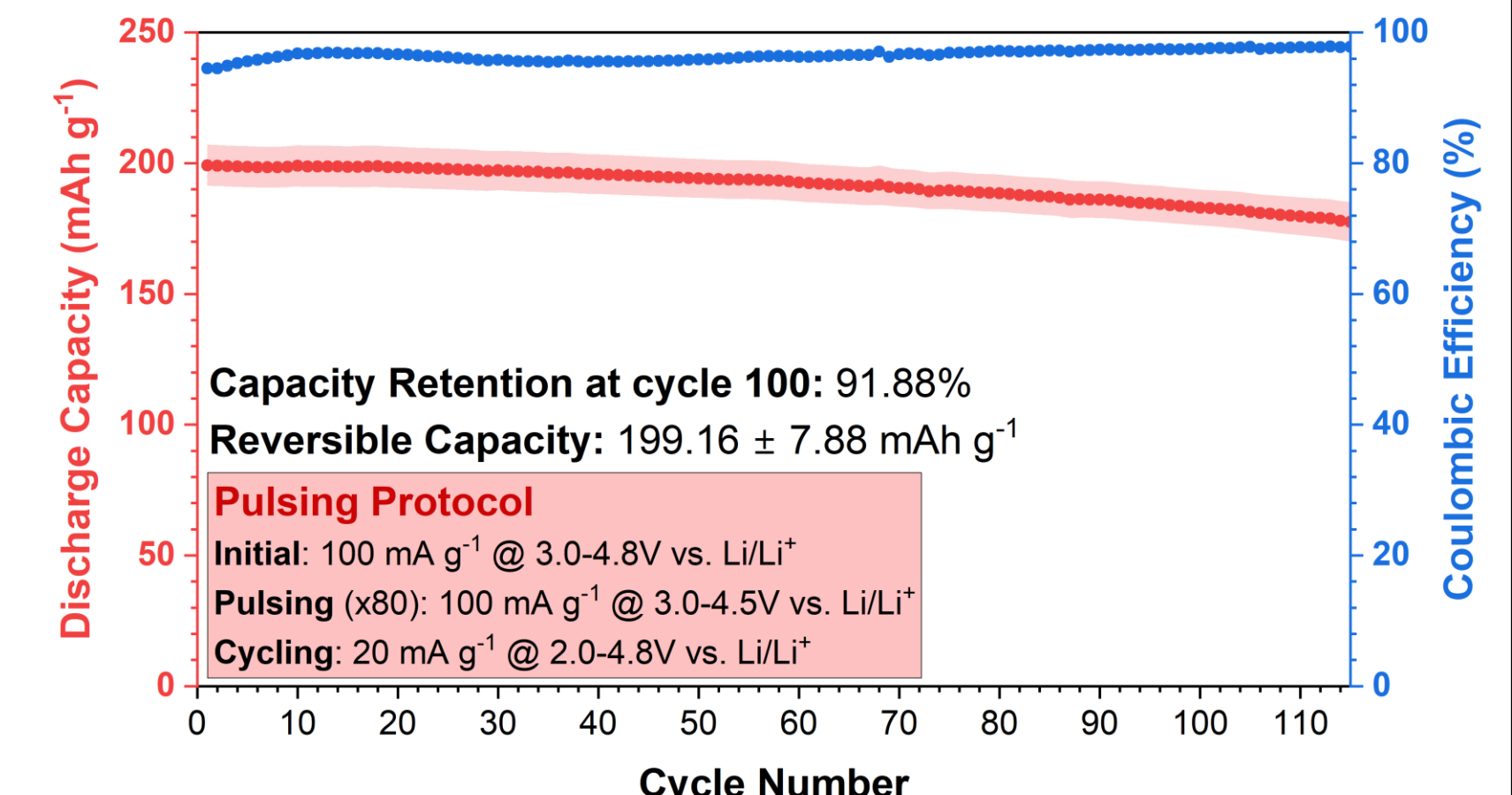
1100°C Synthesis 120°C min⁻¹ quench



$\text{Li}_{1.1}\text{Mn}_{0.8}\text{Ti}_{0.1}\text{O}_{1.9}\text{F}_{0.1}$ 99.35%
 LiMnO_2 0.47%
 LiMn_2O_4 0.18%

- Solid-state synthesis yields $\text{Li}_{1.1}\text{Mn}_{0.8}\text{Ti}_{0.1}\text{O}_{1.9}\text{F}_{0.1}$ DRX (LMTF1811)
- Quench rate affects DRX phase purity when sintering to 1000°C
- 1100°C yields highest phase-pure DRX with insignificant quench rate effect

Electrochemical Performance



Discharge Capacity (mAh g⁻¹)

Cycle Number

Capacity Retention at cycle 100: 91.88%

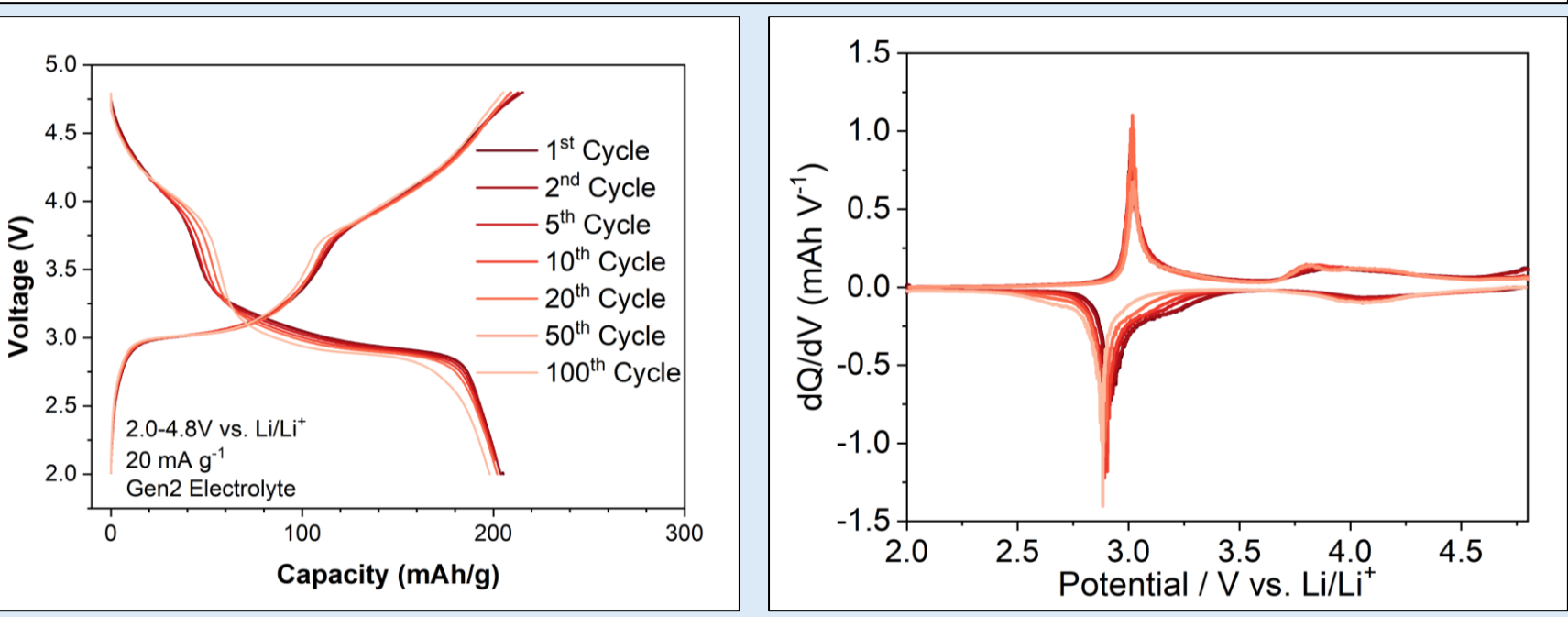
Reversible Capacity: 199.16 \pm 7.88 mAh g⁻¹

Pulsing Protocol

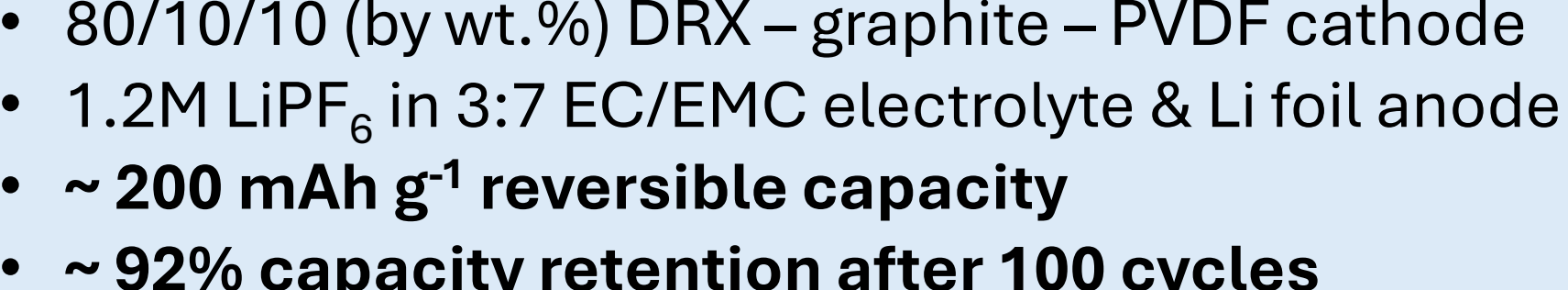
Initial: 100 mA g⁻¹ @ 3.0-4.8V vs. Li/Li⁺

Pulsing (x80): 100 mA g⁻¹ @ 3.0-4.5V vs. Li/Li⁺

Cycling: 20 mA g⁻¹ @ 2.0-4.8V vs. Li/Li⁺



Coulombic Efficiency (%)



Voltage (V)

Capacity (mAh/g)

1st Cycle

2nd Cycle

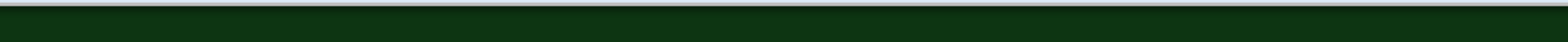
5th Cycle

10th Cycle

20th Cycle

50th Cycle

100th Cycle



dQ/dV (mAh V⁻¹)

Potential / V vs. Li/Li⁺

- 80/10/10 (by wt. %) DRX – graphite – PVDF cathode
- 1.2M LiPF₆ in 3:7 EC/EMC electrolyte & Li foil anode
- ~ 200 mAh g⁻¹ reversible capacity
- ~ 92% capacity retention after 100 cycles

Conclusions

- 2-step synthesis successfully produces **phase-pure LMTF1811 DRX**.
- Combustion precursor yields ideal particle morphology** for cathodes (nanocrystalline aggregates).
- Solid-state reaction produces **high DRX phase purity at 1100°C**, but large DRX particles have **complex, non-ideal morphology**.
- Synthesized DRX shows **promising reversible capacity and retention** with long-term cycling.

Next Steps

- Rapid anneal and quench** for solid-state synthesis.
- Add Li and produce DRX **directly from the combustion synthesis**.
- Adjust combustion fuel ratio** to produce ideal nanocrystalline agglomerates.

Acknowledgements & References

This work is financially supported by the US Department of Energy (DOE) through the DRX+ Consortium which is funded in the Vehicle Technologies Office (VTO) under the Office of Energy Efficiency and Renewable Energy (EERE). SEM imaging was conducted at the Center for Nanophase Materials Sciences (CNMS), which is a DOE Office of Science User Facility.

Darbar, D.; Malkowski, T.; Self, E.C.; Bhattacharya, I.; Reddy, M.V.V.; Nanda, J. An overview of cobalt-free, nickel-containing cathodes for Li-ion batteries. *Materials Today Energy*. 2022, 30, 101173.
 K. Momma and F. Izumi, "VESTA 3 for three-dimensional visualization of crystal, volumetric and morphology data," *J. Appl. Crystallography*, 44, 1272-1276 (2011).
 Chambers, M.S.; Li, T.; Liang, Z.; Kaum, J.; Stone, K.H.; Clément, R.J.; Armstrong, B.L.; Self, E.C. Exploring a new synthesis route to lithium-excess disordered rock salt (DRX) cathode materials. *Materials Advances*. 2025, 6(9), 2990-3001.
 T. Holstun, T. P. Mishra, L. Huang, H.M. Hau, S. Anand, X. Yang, C. Ophus, K. Bustillo, L. Ma, S. Ehrlich, G. Ceder. Accelerating the Electrochemical Formation of the δ -Phase in Manganese-Rich Rocksalt Cathodes. *Advanced Materials*. 2024, 37 (6), 2412871.